Suplemento de la Revista Mexicana de Física **4** 021105 (2023) 1–6

Michel parameters for elucidating the neutrinos nature and searching for new physics

J. M. Márquez

Departamento de Física, Centro de Investigación y de Estudios Avanzados del Instituto Politécnico Nacional
Apartado Postal 14-740, 07000 Ciudad de México, México.

Received 2 May 2023; accepted 4 June 2023

We use the most general four-lepton effective interaction Hamiltonian to investigate the impact of massive Dirac and Majorana neutrinos on the leptonic decays of muons and taus. Our analysis encompasses the specific energy and angular distribution of the resulting charged lepton, accounting for both the initial and final polarizations of the charged leptons. Additionally, we identify the emergence of novel generalized Michel parameters and concentrate on the influence of the heavy neutrino masses, which can make significant contributions in cases where new sterile neutrinos exhibit non-negligible mixing. Our analysis reveals that the most promising scenario occurs in the case of τ decays, featuring one heavy neutrino with a mass approximately ranging from 10^2 to 10^3 MeV. In this setting, the discrepancy between the Dirac and Majorana cases could reach an order of magnitude of 10^{-4}, which is significant enough to be detected in present and future experiments.

Keywords: Electroweak precision physics; sterile or heavy neutrinos.

DOI: https://doi.org/10.31349/SuplRevMexFis.4.021105

1. Introduction

A crucial approach to exploring a fundamental understanding of nature beyond the standard model (SM) is to conduct high-precision measurements, where any potential new physics (NP) could manifest as a noticeable deviation from the SM's prediction, see *e.g.* Refs. [1–3].

In this paper, which is based on Ref. [4], we investigate the leptonic decays $\ell^- \to \ell'^- \bar{\nu}_{\ell'} \nu_\ell$, where the lepton pair (ℓ,ℓ') may be (μ,e), (τ,e), or (τ,μ). Our analysis employs the most general four-lepton effective interaction Hamiltonian to test the SM predictions and to explore potential new physics in the weak charged currents, as well as the impact of neutrino masses and their specific nature. This is particularly relevant in the context of low-scale seesaw scenarios, where the new sterile sectors exhibit non-negligible mixings, and some of them require low enough masses to be produced on-shell, resulting in a detectable effect on the process.

The paper is organized as follows: in Sec. 2, we briefly review the standard Michel distribution in the case of massless neutrinos. We then proceed to compute the effective decay rate, incorporating the finite neutrino masses of Dirac (Sec. 3.1) and Majorana (Sec. 3.2) types in Sec. 3. We summarize both results in a single expression in Sec. 3.3. In Sec. 4, we compare and contrast the common factors and primary differences between the two distributions. Finally, we provide a summary of our findings and some conclusions in Sec. 5.

2. Michel Distribution for Massless Neutrinos

We consider the leptonic decays $\ell^- \longrightarrow \ell'^- \bar{\nu}_{\ell'} \nu_\ell$, for massless neutrinos.

The most general, local, derivative-free, lepton-number conserving, four-lepton interaction Hamiltonian, consistent with locality and Lorentz invariance is [1, 5, 6]

$$\mathcal{H} = 4\frac{G_{\ell\ell'}}{\sqrt{2}} \sum_{n,\epsilon,\omega} g^n_{\epsilon\omega} \left[\bar{\ell}'_\epsilon \Gamma^n (\nu_{\ell'})_\sigma\right] \left[(\bar{\nu}_\ell)_\lambda \Gamma_n \ell_\omega\right]. \quad (1)$$

The subindices ϵ, ω, σ, and λ indicate the chiralities for left (L) and right (R) handed fermions, while $n = S, V, T$ specifies the type of interaction: scalar ($\Gamma^S = I$), vector ($\Gamma^V = \gamma^\mu$), and 'tensor' ($\Gamma^T = \sigma^{\mu\nu}/\sqrt{2}$). Note that tensor interactions can only contribute for opposite chiralities of the charged leptons, which means that only 10 complex coupling constants can appear in the Hamiltonian (4 scalar, 4 vector, and 2 tensor).

After removing an unphysical global phase, we are left with 19 real numbers to be extracted from the experiment. Additionally, the factor $G_{\ell\ell'}$, which is determined from the total decay rate, leads to the following normalization condition for the coupling constants:

$$1 = \frac{1}{4}(|g^S_{RR}|^2 + |g^S_{RL}|^2 + |g^S_{LR}|^2 + |g^S_{LL}|^2) + 3(|g^T_{LR}|^2 + |g^T_{RL}|^2) + (|g^V_{RR}|^2 + |g^V_{RL}|^2 + |g^V_{LR}|^2 + |g^V_{LL}|^2). \quad (2)$$

This results in the theoretical upper-limits: $|g^S_{\epsilon\omega}| \leq 2$,$|g^V_{\epsilon\omega}| \leq 1$ and $|g^T_{\epsilon\omega}| \leq 1/\sqrt{3}$. The Standard Model predicts $|g^V_{LL}| = 1$ with all other couplings being zero. Working with this Hamiltonian, in the massless neutrinos case, the differential decay probability to obtain a final charged lepton with (reduced) energy between $x = E_{\ell'}/\omega$ and $x + dx$, emitted in the direction $\hat{z}$ at an angle between θ and $\theta + d\theta$ with respect to the initial lepton polarization vector $\vec{\mathcal{P}}$, and with its spin parallel to the arbitrary direction $\hat{\zeta}$, neglecting radiative corrections, is given by [7]

$$\frac{d\Gamma}{dx d\cos\theta} = \frac{m_\ell}{4\pi^3}\omega^4 G_{\ell\ell'}^2\sqrt{x^2-x_0^2} \times \Big(F(x) - \frac{\xi}{3}\mathcal{P}\sqrt{x^2-x_0^2}\cos\theta A(x)\Big) \times \big[1+\hat{\zeta}\cdot\vec{\mathcal{P}}_{\ell'}(x,\theta)\big], \quad (3)$$

where $\mathcal{P}=|\vec{\mathcal{P}}|$, $\omega \equiv (m_\ell^2+m_{\ell'}^2)/2m_\ell$, $x_0 \equiv m_{\ell'}/\omega$ and the polarization vector $\vec{\mathcal{P}}_{\ell'}$ in Eq. (3) is

$$\vec{\mathcal{P}}_{\ell'} = P_{T_1}\,\hat{x} + P_{T_2}\,\hat{y} + P_L\,\hat{z}, \quad (4)$$

where $\hat{x},\hat{y}$ and $\hat{z}$ are unit vectors defined as: $\hat{z}$ is along the $\ell^{'}$ momentum $\vec{p}_{\ell'}$, $\hat{z}\times\vec{\mathcal{P}}_{\ell'}/|\hat{z}\times\vec{\mathcal{P}}_{\ell'}| = \hat{y}$ is transverse to $\vec{p}_{\ell'}$ and perpendicular to the decay plane, $\hat{y}\times\hat{z}=\hat{x}$ is transverse to $\vec{p}_{\ell'}$ and in the decay plane, and the components of $\vec{\mathcal{P}}_{\ell'}$ are, respectively

$$P_{T_1}=\mathcal{P}\sin\theta\cdot F_{T_1}(x)\Big/\Big\{F(x)-\frac{\xi}{3}\mathcal{P}\sqrt{x^2-x_0^2}\cos\theta A(x)\Big\},$$
$$P_{T_2}=\mathcal{P}\sin\theta\cdot F_{T_2}(x)\Big/\Big\{F(x)-\frac{\xi}{3}\mathcal{P}\sqrt{x^2-x_0^2}\cos\theta A(x)\Big\},$$
$$P_L=\frac{-F_{IP}(x)+\mathcal{P}\cos\theta\cdot F_{AP}(x)}{F(x)-\frac{\xi}{3}\mathcal{P}\sqrt{x^2-x_0^2}\cos\theta A(x)}, \quad (5)$$

where the explicit form of all these functions can be found in Ref. [7]. These are written in terms of the Michel parameters $\rho,\eta,\delta,\xi,\eta^{''},\xi^{'},\xi^{''},\alpha^{'},\beta^{'}$, which are bilinear combinations of the $g_{\epsilon\omega}^n$ couplings [1,5,7–9]. This final charged-lepton distribution could be used to reveal the signature of NP. Specifically, in the SM case: $\rho=\delta=3/4$, $\eta=\eta^{''}=\alpha^{'}=\beta^{'}=0$ and $\xi=\xi^{'}=\xi^{''}=1$.

The most accurate experimental values on the τ and μ decay Michel parameters [10–16] are shown in Table I. We note that lepton universality yields the most precise η bound from the combination of tau decays into the muon and the electron channel, $\eta = 0.013 \pm 0.020$.

TABLE I. Michel parameters determinations [10–16].

	$\mu^- \to e^-\nu_\mu\bar{\nu}_e$	$\tau^- \to e^-\nu_\tau\bar{\nu}_e$	$\tau^- \to \mu^-\nu_\tau\bar{\nu}_\mu$
ρ	0.74979 ± 0.00026	0.747 ± 0.010	0.763 ± 0.020
η	0.057 ± 0.034	—	0.094 ± 0.073
ξ	$1.0009^{+0.0016}_{-0.0007}$	0.994 ± 0.040	1.030 ± 0.059
$\xi\delta$	$0.7511^{+0.0012}_{-0.0006}$	0.734 ± 0.028	0.778 ± 0.037
$\xi^{'}$	1.00 ± 0.04	—	—
$\xi^{''}$	0.65 ± 0.36	—	—

The interested reader is addressed to Refs. [1, 7] for a detailed discussion.

3. Michel Distribution for Massive Neutrinos

In this context, the interaction of the charged weak current is expressed in the mass eigenstates basis of the charged leptons ℓ and the neutrinos N_j, obtained after diagonalizing the charged lepton and neutrino mass matrices. We work in the basis where the charged lepton mass matrix is already diagonal, where the lepton flavor neutrino basis $\nu_{L,R}$ is assumed to be a superposition of the mass-eigenstate neutrinos N_j with mass m_j, *i.e.*,

$$\nu_{\ell L} = \sum_j U_{\ell j} N_{jL}, \quad \nu_{\ell R} = \sum_j V_{\ell j} N_{jR}, \quad (6)$$

where $j=\{1,2,...,n\}$ labels the number of mass-eigenstate neutrinos.

As shown by Langacker and London [17], explicit lepton-number nonconservation still leads to a matrix element equivalent to the one derived from Eq. (1).

3.1. The Effective Decay Rate for Dirac Neutrinos

The effective Hamiltonian, written in the mass basis, for the $\ell^- \to \ell^{'-}\overline{N}_j N_k$ process is:

$$\mathcal{H} = 4\frac{G_{\ell\ell'}}{\sqrt{2}}\sum_{j,k}\Big\{ g_{LL}^S\Big[\bar{\ell}_L^{'} V_{\ell' j} N_{jR}\Big]\Big[\overline{N}_{kR} V_{\ell k}^* \ell_L\Big] + g_{LL}^V\Big[\bar{\ell}_L^{'}\gamma^\mu U_{\ell' j} N_{jL}\Big]\Big[\overline{N}_{kL} U_{\ell k}^*\gamma_\mu \ell_L\Big] + g_{RR}^S\Big[\bar{\ell}_R^{'} U_{\ell' j} N_{jL}\Big]\Big[\overline{N}_{kL} U_{\ell k}^* \ell_R\Big]$$
$$+ g_{RR}^V\Big[\bar{\ell}_R^{'}\gamma^\mu V_{\ell' j} N_{jR}\Big]\Big[\overline{N}_{kR} V_{\ell k}^*\gamma_\mu \ell_R\Big] + g_{LR}^S\Big[\bar{\ell}_L^{'} V_{\ell' j} N_{jR}\Big]\Big[\overline{N}_{kL} U_{\ell k}^* \ell_R\Big] + g_{LR}^V\Big[\bar{\ell}_L^{'}\gamma^\mu U_{\ell' j} N_{jL}\Big]\Big[\overline{N}_{kR} V_{\ell k}^*\gamma_\mu \ell_R\Big]$$
$$+ g_{LR}^T\Big[\bar{\ell}_L^{'}\frac{\sigma^{\mu\nu}}{\sqrt{2}} V_{\ell' j} N_{jR}\Big]\Big[\overline{N}_{kL} U_{\ell k}^*\frac{\sigma_{\mu\nu}}{\sqrt{2}}\ell_R\Big] + g_{RL}^S\Big[\bar{\ell}_R^{'} U_{\ell' j} N_{jL}\Big]\Big[\overline{N}_{kR} V_{\ell k}^* \ell_L\Big] + g_{RL}^V\Big[\bar{\ell}_R^{'}\gamma^\mu V_{\ell' j} N_{jR}\Big]\Big[\overline{N}_{kL} U_{\ell k}^*\gamma_\mu \ell_L\Big]$$
$$+ g_{RL}^T\Big[\bar{\ell}_R^{'}\frac{\sigma^{\mu\nu}}{\sqrt{2}} U_{\ell' j} N_{jL}\Big]\Big[\overline{N}_{kR} V_{\ell k}^*\frac{\sigma_{\mu\nu}}{\sqrt{2}}\ell_L\Big]\Big\}. \quad (7)$$

For the Dirac neutrinos case $\overline{N}$ represents an antineutrino, then we will have only one possible first-order Feynman diagram. If we define the amplitude to be $\mathcal{M}^D_{jk}$ for the process $\ell^- \longrightarrow \ell'^- \overline{N}_j N_k$, then the corresponding differential decay rate is

$$d\Gamma = \sum_{j,k} \frac{(2\pi)^4 \delta^4(p_1 - p_2 - p_3 - p_4)}{2m_\ell} \times \frac{d^3p_2 d^3p_3 d^3p_4}{(2\pi)^3 2E_2 (2\pi)^3 2E_3 (2\pi)^3 2E_4} |\mathcal{M}^D_{jk}|^2, \quad (8)$$

where the sum extends over all energetically allowed neutrino pairs, including the possible heavy sector involved. Section 3.3 provides the detailed expression for the differential decay rate of Dirac neutrinos.

3.2. The Effective Decay Rate for Majorana Neutrinos

For the Majorana neutrinos case $\overline{N}$ should be identified with N (N=N^c=$C\overline{N}^T$), then, unlike the Dirac case, we will have two possible first-order Feynman diagrams, which shall have strong consequences in the amplitude.

Indeed, as it has been pointed out in well-known previous works [18] for Majorana neutrinos the decay modes $\ell^- \to \ell'^- \overline{N}_j N_k$ and $\ell^- \to \ell'^- \overline{N}_k N_j$ yield the same final states for $j \neq k$ as well as for $j = k$ (since $\overline{N_i} = N_i$), and hence the amplitudes must be added coherently. Figure 1 illustrates the two first-order Feynman diagrams for the decay $\ell^- \to \ell'^- N_j N_k$.

The first diagram leads to the same matrix element as the Dirac case, while the second diagram is only possible in the Majorana neutrino case due to the identification of N and $\overline{N}$. The orientation of each fermion chain (indicated by blue arrows) is also defined according to the Feynman rules for Majorana fermions [19].

If we define the total amplitude to be $\mathcal{M}_{jk}$ for the process $\ell^- \to \ell'^- N_j N_k$, then the differential decay rate is

$$d\Gamma = \frac{1}{2} \sum_{j,k} \frac{(2\pi)^4 \delta^4(p_1 - p_2 - p_3 - p_4)}{2m_\ell} \times \frac{d^3p_2 d^3p_3 d^3p_4}{(2\pi)^3 2E_2 (2\pi)^3 2E_3 (2\pi)^3 2E_4} |\mathcal{M}_{jk}|^2. \quad (9)$$

The above equation includes an additional factor of 1/2 for two different reasons. The first one is the usual statistical factor when dealing with indistinguishable fermions for the case where $j = k$. The second reason is due to double counting for the case where $j \neq k$. This is because the sum over j and k is not limited to $j \leq k$.

If $\mathcal{M}^D_{jk}$ and $\mathcal{M}^M_{jk}$ are the amplitudes coming from the first and second diagram respectively, then, once the integration over the momenta of the neutrinos is carried out, the decay rate will have a dependence on the amplitude as follows:[i]

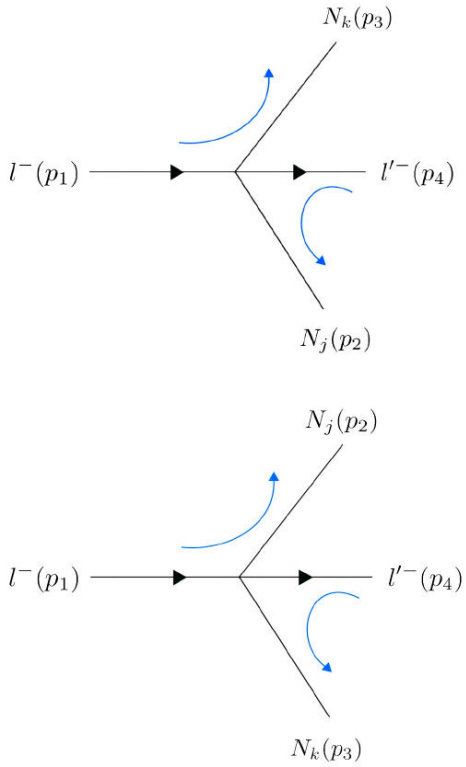

FIGURE 1. First-order Feynman diagrams for $\ell^- \longrightarrow \ell'^- N_j N_k$.

$$\begin{aligned} d\Gamma &\propto \frac{1}{2} \sum_{j,k} |\mathcal{M}^D_{jk} - \mathcal{M}^M_{jk}|^2 \\ &= \frac{1}{2} \sum_{j,k} \left\{ |\mathcal{M}^D_{jk}|^2 + |\mathcal{M}^M_{jk}|^2 - 2\,\mathrm{Re}(\mathcal{M}^D_{jk} \mathcal{M}^{M*}_{jk}) \right\} \\ &= \sum_{j,k} |\mathcal{M}^D_{jk}|^2 - \sum_{j,k} \mathrm{Re}(\mathcal{M}^D_{jk} \mathcal{M}^{M*}_{jk}). \end{aligned} \quad (10)$$

The key difference between the Dirac and Majorana cases is the interference term, which is referred to as the Majorana term [20]. This contribution arises due to the presence of the second Feynman diagram in the Majorana case, and it has an overall minus sign that comes from the application of Wick's theorem when dealing with Majorana fermions [19].

Using this property, we can summarize the Dirac and Majorana cases in a single expression, where the Dirac case is just the result obtained from the Majorana one when we force the Majorana term to vanish. We can do this by the implementation of a flag parameter $\epsilon = 0, 1$, as we shall see next.

3.3. Final Distribution (Dirac and Majorana neutrinos)

Our final distribution will be expressed using the widely used PDG parametrization convention [7]. As previously discussed, to differentiate between the two natures of neutrinos, we incorporate the Majorana term by introducing the parameter $\epsilon = 0, 1$. This approach enhances the clarity and usability of our expressions for various applications.

Then, the differential decay probability taking into account finite Dirac ($\epsilon = 0$) or Majorana ($\epsilon = 1$) neutrino masses is given by

$$\frac{d\Gamma}{dx d\cos\theta} = \sum_{j,k} \frac{m_\ell}{4\pi^3}\omega^4 G^2_{\ell\ell'}\sqrt{x^2-x_0^2}\Big([F_{IS}(x)+F'_{IS}(x)+F''_{IS}(x)] - \mathcal{P}\cos\theta\big[F_{AS}(x)+F'_{AS}(x)+F''_{AS}(x)\big]\Big)\big(1+\hat{\zeta}\cdot\vec{\mathcal{P}}_{\ell'}(x,\theta)\big), \tag{11}$$

and the components of $\vec{\mathcal{P}}_{\ell'}$ are, respectively,

$$\begin{aligned} P_{T_1} &= \mathcal{P}\sin\theta\cdot\big(F_{T_1}(x)+F'_{T_1}(x)+F''_{T_1}(x)\big)\Big/N, \\ P_{T_2} &= \mathcal{P}\sin\theta\cdot\big(F_{T_2}(x)+F'_{T_2}(x)+F''_{T_2}(x)\big)\Big/N, \\ P_L &= \Big(-\big(F_{IP}(x)+F'_{IP}(x)+F''_{IP}(x)\big)+\mathcal{P}\cos\theta\big(F_{AP}(x)+F'_{AP}(x)+F''_{AP}(x)\big)\Big)\Big/N, \end{aligned} \tag{12}$$

with N the normalization factor $N = \big(F_{IS}(x)+F'_{IS}(x)+F''_{IS}(x)\big) - \mathcal{P}\cos\theta\big(F_{AS}(x)+F'_{AS}(x)+F''_{AS}(x)\big)$.

This can be viewed as a simple extension of the massless neutrino case. Specifically, for each standard function, we introduce two additional functions: a primed function and a biprimed function. These functions have linear ($m_\nu/m_{l'}$) and quadratic ($m^2_\nu/m^2_{l'}$) dependence on the neutrino masses, respectively. Their explicit form and the new Michel parameters that arise due to considering finite neutrino masses can be found in Ref. [4], as an example:

$$\begin{aligned} F'_{T_1}(x) &= \frac{1}{4}\frac{m_j}{m_1}\,\mathrm{Re}\left[(\lambda^+_L)_{jk}\Big(x_0(1-x)+x_0\sqrt{1-x_0^2}\Big)-(\lambda^+_R)_{kj}\Big(x\big(1+\sqrt{1-x_0^2}\big)-x_0^2\Big)\right], \\ (\lambda^+_N)_{jk} &= -(f^S_{NN})_{jk}(f^V_{LR})^*_{jk}+(f^V_{NN})_{jk}((f^S_{LR})^*_{jk}+2(f^T_{LR})^*_{jk})+2(f^S_{NN})_{kj}(f^T_{LR})^*_{kj}-2(f^V_{NN})_{kj}(f^V_{LR})^*_{kj} \\ &\quad+\epsilon\Big[-2(f^V_{NN})_{kj}(f^V_{LR})^*_{jk}+\frac{1}{2}(f^S_{NN})_{kj}(f^S_{LR})^*_{jk}+(f^S_{NN})_{kj}(f^T_{LR})^*_{jk}+4(f^V_{NN})_{jk}(f^T_{LR})^*_{kj} \\ &\quad-(f^S_{NN})_{jk}(f^V_{LR})^*_{kj}\Big]+(L\leftrightarrow R), \end{aligned} \tag{13}$$

where the f^n_{lm} constants are related to the g^n_{lm} couplings via the neutrinos mixing matrix elements, as can be seen in Ref. [4]. The specific neutrino mass suppression and the presence of new parameters is evident. Also, we distinguish the specific Majorana term in every parameter with the parameter ϵ, being $\epsilon = 0(1)$ for Dirac (Majorana) case as we just wanted.

4. Dirac vs Majorana distribution

Both the Dirac and Majorana distributions exhibit the same suppression due to neutrino masses. We can estimate it and evaluate its impact on the spectrum. To simplify the analysis, we will consider only one additional heavy neutrino and focus on the suppression resulting from its mass and mixing.

If the heavy neutrino is within reach kinematically, the suppression of the terms featuring explicit dependence on neutrino masses in the primed and biprimed functions will be affected by the mass of the heavy neutrino and its interaction with the active and sterile sectors.

We estimate this suppression for the general case, taking into account one and two final heavy neutrinos, where the suppression is computed as $|U_{\ell 4}|^2(m_\nu/m_\ell)$ and $|U_{\ell 4}|^2|U_{\ell' 4}|^2(m_\nu/m_\ell)^2$ for the linear and quadratic terms respectively, where the specific neutrino mass and mixing are taken from the best experimental constraints on an invisible heavy neutrino [21, 22]. Taking these factors into account, we can calculate the level of suppression of the terms that depend on the neutrino mass compared to those without such dependence, the most relevant case is shown in Table II.

These findings are intriguing because they suggest that a heavy neutrino sector with a mass of around $10^2 - 10^3$ MeV could produce significant distortions of the order of $\mathcal{O}(10^{-3})$ in the differential decay rate of a τ-decay. This further underscores the importance of exploring new physics in this process.

So far, we have only considered the effects of neutrino masses and mixings and have not accounted for the impact

TABLE II. Suppression of neutrino mass dependent terms.

Neutrino	Mass (GeV)	Mixing Suppression	Linear Term Suppression
Heavy (1) ($\ell = \tau$)	$0.1 - 1.2$	$10^{-7} - 10^{-3}$	$10^{-8} - 10^{-3}$

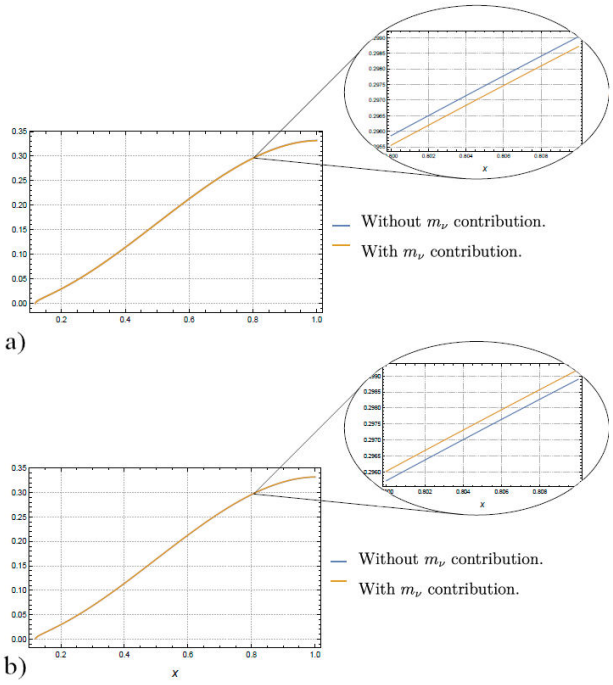

FIGURE 2. a) Neutrino mass effect on the Dirac, and b) Majorana energy spectrum of the final charged-lepton.

of the new physics couplings. To provide a more realistic assessment of the potential effects of a heavy neutrino sector, we apply our results to an example model that considers the dominant g^V_{LL} coupling and a non-zero g^S_{RR}, still with left-handed neutrinos. This coupling is among the most well-motivated new physics interactions and naturally arises in many beyond SM theories. Additionally, to prevent the linear neutrino mass terms from vanishing, we introduce another non-vanishing coupling, g^S_{LR}, in our simple yet realistic example of a scalar NP sector. The specific dependence of the new Michel parameters can be seen in Ref. [4].

By using the experimental mean values for the standard Michel parameters and assigning numerical values of $g^V_{LL} = 0.96$, $g^S_{RR} = 0.25$, and $g^S_{LR} = 0.5$ for the new parameters in the tau lepton case, which adhere to the normalization condition and also meet the current restrictions on the couplings, it is possible to obtain the energy spectrum for both the Dirac and Majorana cases, with and without the inclusion of neutrino mass contributions, which is presented in Fig. 2.

The plot in Fig. 2 illustrates that the overall impact of the net neutrino mass could be around 10^{-4}. This means that even after factoring in the suppression of the relevant new physics couplings and phase space structures, the influence of the neutrino mass could still cause noticeable alterations in the energy spectrum.

Also, for this realistic example, we have discovered that the neutrino mass has a specific impact on the energy distribution for the Dirac and Majorana scenarios, producing opposing effects. Indeed for Dirac neutrinos, the neutrino mass leads to a decrease in the differential decay rate, whereas for

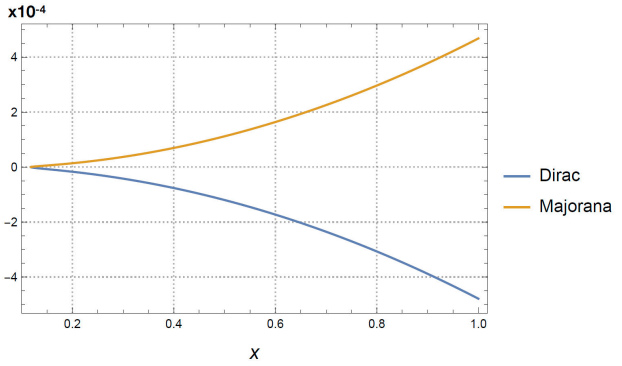

FIGURE 3. Neutrino mass contribution to energy distributions in Dirac and Majorana cases.

Majorana neutrinos, it leads to an increase in the differential decay rate.

Actually, to derive the precise impact of the neutrino mass term in the Dirac and Majorana cases, we can compute the difference between the differential rate with neutrino mass effects and the rate without this contribution. As shown in Fig. 3, our findings align with the prior discussion, indicating an opposing net effect in the Dirac and Majorana rates that is of the order of 10^{-4}.

Therefore, the alteration of the energy spectrum, if observed, could serve the dual purpose of identifying the existence of a heavy neutrino sector and distinguishing between the Dirac and Majorana nature of neutrinos.

Also, the interference Majorana term, which affects every Dirac parameter, could generate a measurable distortion depending on the new physics involved. Thus, studying this term via the ϵ parameter could provide another way to distinguish the neutrino nature and the presence of new physics.

A complete analysis can be found in Ref. [4], where we apply our expressions to other model dependent scenarios, reproducing well-known results and discussing their main properties.

5. Summary and Conclusions

In this work, the decay process $\ell^- \to \ell'^- N_j N_k$ has been studied, where N_j and N_k represent mass-eigenstate neutrinos. The matrix element of this decay has been derived using the general four-lepton effective interaction Hamiltonian, and the resulting energy and angular distribution of the final charged lepton has been calculated, along with the polarization of both the decaying and final charged leptons.

By introducing generalized Michel parameters and a flag parameter $\epsilon = 0, 1$, we were able to classify the Dirac and Majorana contributions in a single result. Our results are presented in a general form, making them applicable to model-dependent scenarios and facilitating the differentiation of the possible nature of neutrinos.

We analyze the properties and distinctions of the decay rate for both the Dirac and Majorana scenarios, and determine the magnitude of the neutrino mass dependent contributions

based on some of the best experimental constraints on an invisible heavy neutrino, where in the case of a τ-decay featuring a single massive final-state neutrino with a mass range of $10^2 - 10^3$ MeV, the suppression from the linear term could be around 10^{-4}, which is a sufficiently low value to be detectable in ongoing and upcoming experiments.

Acknowledgement

The author wishes to thank the organizers for the pleasant conference. Conacyt funding his Ms. Sc. and Ph. D. is also acknowledged, together with Gabriel López Castro and Pablo Roig for useful guidance.

---

i. It is worth noting that once the momenta of the neutrinos are integrated out, $\mathcal{M}^D_{jk}$ and $\mathcal{M}^M_{jk}$ are related to each other through the exchange $j \leftrightarrow k$.

1. A. Pich, Precision Tau Physics *Prog. Part. Nucl. Phys.* **75** (2013) 41, https://doi.org/10.1016/j.ppnp.2013.11.002
2. A. Pich, *Precision tests of the Standard Model* (1997), https://doi.org/10.48550/arXiv.hep-ph/9711279
3. T. P. Gorringe, and D. W. Hertzog, *Precision Muon Physics* (2015), Prog.Part.Nucl.Phys. **84** (2015) 73, https://doi.org/10.48550/arXiv.1506.01465
4. J. M. Márquez, G. L. Castro, and P. Roig, *Michel parameters in the presence of massive Dirac and Majorana neutrinos.* JHEP **11** (2022) 117, https://doi.org/10.1007/JHEP11%282022%29117
5. L. Michel, *Interaction between four half spin particles and the decay of the μ meson*, Proc. Phys. Soc. **A 63** (1950) 1371, https://doi.org/10.1088/0370-1298/63/5/311
6. C. Bouchiat and L. Michel, *Theory of μ-Meson Decay with the Hypothesis of Nonconservation of Parity*, Phys. Rev. **106** (1957) 170, https://doi.org/10.1103/PhysRev.106.170
7. Particle Data Group, *Review of Particle Physics*, **PTEP 2022** (2022) 083C01, https://doi.org/10.1093/ptep/ptac097
8. W. Fetscher, *Helicity dependence of the electron-neutrino energy spectrum from the decay of unpolarized muons*, Phys. Rev. D **49** (1994) 5945, https://doi.org/10.1103/PhysRevD.49.5945
9. C. A. Gagliardi, R. E. Tribble, and N. J. Williams, Global analysis of muon decay measurements *Phys. Rev. D* **72** (2005) 073002, https://doi.org/10.1103/PhysRevD.72.073002
10. K. Abe *et al*. (SLD Collaboration), Measurement of the tau-neutrino he- licity and the Michel parameters in polarized e^+e^- collisions, *Phys. Rev. Lett.* **78** (1997) 4691, https://doi.org/10.1103/PhysRevLett.78.4691.
11. A. Heister *et al*. (ALEPH Collaboration), Measurement of the Michel parameters and the nu/tau helicity in tau lepton decays, *Eur. Phys. J. C* **22** (2001) 217, https://doi.org/10.1007/s100520100813.
12. P. Abreu *et al*., (DELPHI Collaboration), A Study of the Lorentz structure in tau decays, *Eur. Phys. J. C* **16** (2000) 229, https://doi.org/10.1007/s100520050017
13. K. Ackerstaff *et al*., (OPAL Collaboration), Measurement of the Michel parameters in leptonic tau decays, *Eur. Phys. J. C* **8** (1999) 3, https://doi.org/10.1007/s100529901080
14. M. Acciarri *et al*., L3 Collaboration, Measurement of the Michel parameters and the average tau-neutrino helicity from tau decays at LEP, *Phys. Lett. B* **438** (1998) 405, https://doi.org/10.1016/S0370-2693(98)01082-X
15. H. Albrecht *et al.*, ARGUS Collaboration, Determination of the Michel parameters rho, xi and delta in tau lepton decays with tau $\longrightarrow$ rho neutrino tags, *Phys. Lett. B* **431** (1998) 179, https://doi.org/10.1016/S0370-2693%2898%2900565-6
16. J. P. Alexander *et al.*, (CLEO Collaboration), Determination of the Michel parameters and the tau-neutrino helicity in tau decay, *Phys. Rev. D* **56** (1997) 5320, https://doi.org/10.1103/PhysRevD.56.5320
17. P. Langacker and D. London, Analysis of Muon Decay With Lepton Number Nonconserving Interactions, *Phys. Rev. D* **39** (1989) 266, https://doi.org/10.1103/PhysRevD.39.266
18. R. E. Shrock, Pure Leptonic Decays With Massive Neutrinos And Arbitrary Lorentz Structure, *Phys. Lett. B* **112** (1982) 382, https://doi.org/10.1016/0370-2693(82)91074-7
19. A. Denner, H. Eck, O. Hahn, and J. Kublbeck, Feynman rules for fermion number violating interactions, *Nucl. Phys. B* **387** (1992) 467, https://doi.org/10.1016/0550-3213(92)90169-C
20. M. Doi, T. Kotani and E. Takasugi, Double Beta Decay and Majorana Neutrinos, *Progress of Theoretical Physics Supplement*, **83** (1985) 83.1, https://doi.org/10.1143/PTPS.83.1
21. A. de Gouvea, and A. Kobach, Global Constraints on a Heavy Neutrino *Phys. Rev. D* **93** (2016) 033005, https://doi.org/10.1103/PhysRevD.93.033005
22. A. Kobach and S. Dobbs, Heavy Neutrinos and the Kinematics of Tau Decays *Phys. Rev. D* **91** (2015) 053006, https://doi.org/10.1103/PhysRevD.91.053006